Pattern Recognition 45 (2012) 3810–3824

Contents lists available at SciVerse ScienceDirect

Pattern Recognition

journal homepage: www.elsevier.com/locate/pr

Two-dimensional histogram equalization and contrast enhancement ☆

Turgay Celik [a,b,*]

[a] Bioinformatics Institute, A*STAR (Agency for Science, Technology and Research), 30 Biopolis Street, #07-01, Matrix, Singapore 138671
[b] Electrical and Electronics Engineering, Meliksah University, 38280 Talas/Kayseri, Turkey

ARTICLE INFO

Article history:
Received 27 November 2010
Received in revised form
19 January 2012
Accepted 21 March 2012
Available online 4 April 2012

Keywords:
Contrast enhancement
Histogram equalization
Image quality enhancement

ABSTRACT

In this paper, we propose a two-dimensional histogram equalization (2DHE) algorithm which utilizes contextual information around each pixel to enhance the contrast of an input image. The algorithm is based on the observation that the contrast in an image can be improved by increasing the grey-level differences between each pixel and its neighbouring pixels. The image equalization is achieved by assuming that for a given image, the modulus of the grey-level differences between pixels and their neighbouring pixels are equally distributed. The well-known global histogram equalization algorithm is a special case of 2DHE when contextual information is not utilized. 2DHE is easy to implement requiring only a small number of simple arithmetic operations and is thus suitable for real-time contrast enhancement applications. Experimental results show that 2DHE produces better or comparable enhanced images than several state-of-the-art algorithms. The only parameter in 2DHE which requires tuning is the size of the spatial neighbourhood support which provides the contextual information for a given dynamic range of the enhanced image. An automated parameter selection algorithm is also presented. The algorithm can be applied to a wide range of image types.

1. Introduction

Contrast enhancement of digital images is used to process an input image such that the visual content of the output image is more pleasing or more useful for machine vision applications. However, choosing an appropriate contrast enhancement algorithm is not an easy task due to the lack of the dependable measures to quantify the output image quality. Furthermore, enhancement algorithms usually rely on proper parameter selection which also suffers from lack of the dependable measures. To solve these problems, there are a large number of enhancement algorithms that have been proposed in the literature.

Contrast enhancement algorithms can be categorized into two major groups according to the data domain they are applied to: (1) transform-domain algorithms; and (2) image-domain algorithms. Transform-domain algorithms decompose an input image into different subbands so as to modify, globally or locally, the magnitude of the desired frequency components of the image data using multiscale analysis [1–4]. These algorithms enable the simultaneous global and local contrast enhancement by transforming the appropriate subbands and in the appropriate scales. The algorithms are computationally complex, and in order to avoid degrading the image, they require appropriate settings of the associated parameters. For example, the centre-surround Retinex [1] algorithm was developed to achieve lightness and colour constancy in images, where constancy refers to the perception of colour and lightness invariant to spatial and spectral illumination variations. The enhanced image has the benefits of compressed dynamic range and colour independent of the spatial distribution of the scene illumination. However, the enhanced image may include "halo" artefacts, especially along boundaries between large uniform regions. A "greying out" can also occur resulting in the image of the scene tending to middle grey. Second-generation wavelets are used to produce enhanced images without "halo" artefacts. In edge-avoiding wavelets based contrast enhancement algorithm (EAW) [4], the wavelet coefficients in transform domain are modified and inverse transform is applied to obtain contrast enhanced images. The method achieves both global and local contrast enhancement at the same time with a proper parameter selection.

Although the transform-domain contrast enhancement algorithms had shown promising results in a variety of problem domains, image-domain contrast enhancement algorithms are widely used. Among image-domain algorithms, global histogram equalization (HE) remains as one of the most popular techniques for its implementation simplicity and satisfactory performance in general [5]. HE uses an input-to-output mapping derived from the cumulative distribution function (CDF) of the input image

☆This work is supported by the Agency for Science, Technology, and Research (A*STAR) of Singapore.

* Correspondence address: Bioinformatics Institute, A*STAR (Agency for Science, Technology and Research), 30 Biopolis Street, #07-01, Matrix, Singapore 138671. Tel.: +65 9800 1377.
E-mail address: celikturgay@gmail.com

0031-3203/$ - see front matter © 2012 Elsevier Ltd. All rights reserved.
http://dx.doi.org/10.1016/j.patcog.2012.03.019

histogram. The CDF of the input image is mapped to the CDF of the uniform distribution. The mapping causes grey levels with large pixel populations to be expanded to occupy a larger range of grey levels while the other grey-level ranges with fewer pixels are compressed to smaller ranges. Although HE utilizes the available grey scale of the image efficiently, it tends to over-enhance the image contrast if there are large peaks in the histogram, resulting in a harsh and noisy appearance of the enhanced image. HE do not always produce satisfactory enhancement, especially for images with large spatial variation in contrast. HE also tends to over-emphasize any noise in an image.

Local histogram equalization (LHE) based enhancement algorithms have been developed, e.g., [6,7], to address the aforementioned problems. The LHE in [7] uses a small window that slides through every image pixel sequentially and the histogram of pixels within the current position of the window is equalized. The grey-level mapping for enhancement is applied only to the centre pixel of the window. LHE sometimes over-enhances some portion of the image and enhances any noise along with the image features. LHE based algorithms also produce undesirable checkerboard effects. The computational complexity of LHE based algorithms and their requirement for window size selection have led researchers to improve the performance of HE using alternative algorithms. Algorithms that focus on improving HE include brightness preserving bi-histogram equalization (BBHE) [8], equal area dualistic sub-image histogram equalization (DSIHE) [9], minimum mean brightness error bi-histogram equalization (MMBEBHE) [10], and minimum within-class variance multi-histogram equalization (MWCVMHE) [11]. BBHE attempts to solve the brightness preservation problem and uses the average grey level of the input image pixels to split the image histogram into two histograms. The two histograms are then independently equalized. Following the same basic ideas used by the BBHE algorithm of decomposing the original image histogram into two sub-histograms and then equalize the sub-histograms, DSIHE splits the input image histogram into two sub-histograms aiming at the maximization of the Shannon's entropy of the output image. MMBEBHE, an extension of BBHE, provides maximal brightness preservation by searching for a threshold level that decomposes the input image histogram into two sub-histograms, such that the minimum brightness difference between the input image and the output image is achieved, whereas the former algorithms consider only the input image to perform the decomposition. Although these algorithms can achieve satisfactory contrast enhancement, the variation in the grey-level distribution may result in annoying side effects [12]. Similar to the above mentioned algorithms, MWCVMHE automatically partitions the input histogram into multiple sub-histograms (each sub-histogram forms a class) by minimizing within-class variance and then applies histogram equalization in each sub-histogram separately. MWCVMHE applies dynamic programming in optimizing a cost function formed from within-class variances to achieve automatic histogram partitioning. It overcomes the performances of the histogram partitioning based algorithms. MWCVMHE achieves brightness preservation which may result in a low-contrast output image.

Optimization algorithms have also been used for contrast enhancement. Convex optimization is used in flattest histogram specification with accurate brightness preservation (FHSABP) [13] to transform the input image histogram into the flattest histogram, subject to a mean brightness constraint. This is followed by applying an exact histogram specification algorithm to preserve the image brightness. FHSABP behaves very similar to HE when the grey levels of the input image are equally distributed or when the average brightness value of the input image is mid point of the dynamic range, i.e., 127.5 when 8-bit data representation is considered. Since it is designed to preserve the average brightness, FHSABP may produce low contrast results when the average brightness is either too low or too high. Contrast enhancement in histogram modification framework (HMF) is treated as an optimization problem that minimizes a cost function [14]. Penalty terms are introduced in the optimization process in order to address noise and black/white stretching. By using different adaptive parameters, HMF can achieve different levels of contrast enhancement. However, these parameters need to be manually adjusted according to the image content to achieve high contrast. In order to design a parameter free contrast enhancement algorithm, genetic algorithm (GA) is employed in [15] to find a target histogram which maximizes a contrast measure based on edge information. We refer this algorithm as contrast enhancement based on GA (CEBGA). CEBGA suffers from the drawbacks of GA based algorithms, namely dependency on initialization and convergence to a local optimum. The mapping to the target histogram is scored only by the maximum contrast, measured using the average edge strength estimated from the gradient information. Thus, the resulting enhancement may not be spatially smooth. Furthermore, the convergence time is proportional to the number of distinct grey levels of the input image.

In this paper, we propose an adaptive image enhancement algorithm named as two-dimensional histogram equalization (2DHE) algorithm which is effective in terms of improving the visual quality of different types of input images. 2DHE has only one parameter to tune, namely the size of the spatial neighbourhood support which provides the contextual information. It only requires a small number of simple arithmetic operations and is thus suitable for real-time applications. The enhancement process is based on the observation that contrast of an image can be improved by increasing the grey-level differences between the pixels of an input image and their neighbours. Furthermore, for the purpose of image equalization, grey-level differences should be equally distributed over the entire input image. To realize these observations, a two-dimensional (2D) histogram of the input image is constructed using mutual relationship between each pixel and its neighbouring pixels. The final mapping between input grey-levels and output grey-levels is achieved by considering 2D input and target histograms. 2DHE is a generalized form of HE. When a single pixel is considered, 2DHE acts as HE. However 2DHE starts to behave differently when the contextual information is considered. A metric which considers discrete entropy and measure of contrast at the same pixel is also proposed to achieve automatic parameter selection for the proposed algorithm.

The paper is organized as follows. Section 2 presents the proposed automatic image equalization algorithm. Section 3 presents the subjective and quantitative comparisons of the proposed algorithm with several state-of-the-art enhancement techniques. Section 4 concludes the paper.

2. Proposed algorithm

2.1. Grey-scale image enhancement

Consider an input image, $\mathbf{X}=\{x(i,j)|1\le i\le H,1\le j\le W\}$, of size $H\times W$ pixels, where $x(i,j)\in[0,\mathbb{Z}^+]$ and assume that $\mathbf{X}$ has a dynamic range of $[x_d,x_u]$ where $x(i,j)\in[x_d,x_u]$. The main objective of the proposed algorithm is to generate an enhanced image, $\mathbf{Y}=\{y(i,j)|1\le i\le H,1\le j\le W\}$, which has a better visual quality than $\mathbf{X}$. The dynamic range of $\mathbf{Y}$ can be stretched or compressed into the interval $[y_d,y_u]$, where $y(i,j)\in[y_d,y_u]$, $y_d<y_u$ and $y_d,y_u\in[0,\mathbb{Z}^+]$.

The conventional approach to enhance the image contrast in an image is to manipulate the grey-level of individual pixels to the required value by constructing a one-dimensional (1D) intensity histogram and then transforming it. However, such an

approach does not take into account the local contextual information content in the image when constructing the histogram. In order to consider contextual information around each pixel, a 2D histogram is created, i.e., for each grey-level of the input image, the distribution of other grey-levels in the neighbourhood of the corresponding pixel is computed.

Let $\mathcal{X}=\{x_1,x_2,\ldots,x_K\}$ be the sorted set of K distinct grey-levels of the input image $\mathbf{X}$ where $x_1<x_2<\ldots<x_K$, $x_1=x_d$, $x_K=x_u$, and the 2D histogram be expressed as

$$\mathbf{H}_x=\{h_x(m,n)\,|\,1\le m\le K,1\le n\le K\}, \tag{1}$$

where $h_x(m,n)\in\mathbb{R}$. The $h_x(m,n)$ is computed as

$$h_x(m,n)=\sum_{\forall i}\sum_{\forall j}\sum_{k=-\lfloor w/2\rfloor}^{\lfloor w/2\rfloor}\sum_{l=-\lfloor w/2\rfloor}^{\lfloor w/2\rfloor}\phi_{m,n}(x(i,j),x(i+k,j+l))(|x_m-x_n|+1), \tag{2}$$

where w is an odd integer number used in parametrizing a square $w\times w$ neighbourhood around each pixel, and $\phi_{m,n}(x(i,j),x(i+k,j+l))\in\{0,1\}$ is a binary function used in identifying the occurrence of the grey-levels x_m and x_n at the spatial locations of (i,j) and $(i+k,j+l)$, respectively, i.e.,

$$\phi_{m,n}(x(i,j),x(i+k,j+l))=\begin{cases}1, & \text{if } x_m=x(i,j) \quad \text{and} \quad x_n=x(i+k,j+l);\\ 0, & \text{otherwise.}\end{cases} \tag{3}$$

The entry $h_x(m,n)$ is the number of occurrences of the nth grey-level (x_n) in the neighbourhood of the mth grey-level (x_m) weighted by their absolute valued differences ($|x_m-x_n|+1$). One is added to the absolute valued difference $|x_m-x_n|$ to avoid giving 0 weight to occurrence of $x_m=x_n$. Eq. (2) assigns higher weights to the entries of the 2D histogram when the difference between x_m and x_n is large, and vice versa. When the contrast of the image is taken into consideration, one expects larger grey-level differences between the pixel under consideration and its neighbours for improved contrast. Hence, the weighting mimics the basic notion of the contrast and favours the combinations of x_m and x_n according to the differences between them.

The elements of the 2D histogram $h_x(m,n)$ is normalized according to

$$h_x(m,n)=h_x(m,n)\Big/\sum_{i=1}^{K}\sum_{j=1}^{K}h_x(i,j) \tag{4}$$

to give a probability distribution which is summed to provide a cumulative distribution as

$$\mathcal{P}_x=\{P_x(m)\,|\,m=1,\ldots,K\}, \tag{5}$$

where

$$P_x(m)=\sum_{i=1}^{m}\sum_{j=1}^{K}h_x(i,j).$$

Different types of local neighbourhood can be employed, however for a typical implementation of the proposed algorithm $w\times w$ square neighbourhood around each pixel is considered. For example, Fig. 1 shows the *House* image and its normalized 2D histograms according to Eq. (4) using different size of local neighbourhoods. The *House* image has more brighter regions, thus its 2D histogram has larger values located at higher grey-values. When the 2D histogram is observed closely, one can see that the diagonal elements of the 2D histogram have larger values. This is mainly due to the homogeneous regions in the image. In homogeneous regions, the neighbours of each pixel have very similar grey-levels which result in higher peaks at diagonal or near-diagonal values of the 2D histogram. As can be observed from Fig. 1(b)–(h), when the size of local neighbourhood gets larger, the more contextual information is utilized. In 2D histogram, peaks around main-diagonal elements are smeared and while regions representing high differences between x_m and x_n are enhanced.

Let $\mathcal{Y}=\{y_1,y_2,\ldots,y_L\}$ be the sorted set of L distinct grey-levels of the output image $\mathbf{Y}$ where $y_1<y_2<\cdots<y_L$, $y_1=y_d$, $y_L=y_u$ for a given output range of $[y_d,y_u]$. In order to map the elements of $\mathcal{X}$ to the elements of $\mathcal{Y}$, one needs to find a 2D target probability distribution function and its cumulative histogram. In a contrast enhanced image, one expects that different combinations of grey-level pairs are equally distributed. Thus, in order to enhance every possible occurrence of grey-levels of input image pixels and their neighbours equally, an optimum 2D uniformly distributed target probability distribution function is formed as

$$\mathbf{H}_t=\{h_t(m',n')=1/L^2\,|\,1\le m'\le L,1\le n'\le L\}, \tag{6}$$

where L is the number of the distinct grey-levels in the range $[y_d,y_u]$, and

$$\sum_{m'=1}^{L}\sum_{m'=1}^{L}h_t(m',n')=1.$$

The target cumulative distribution function formed using the target probability distribution function $h_t(m',n')$ is defined as

$$\mathcal{P}_t=\{P_t(m')\,|\,m'=1,\ldots,L\}, \tag{7}$$

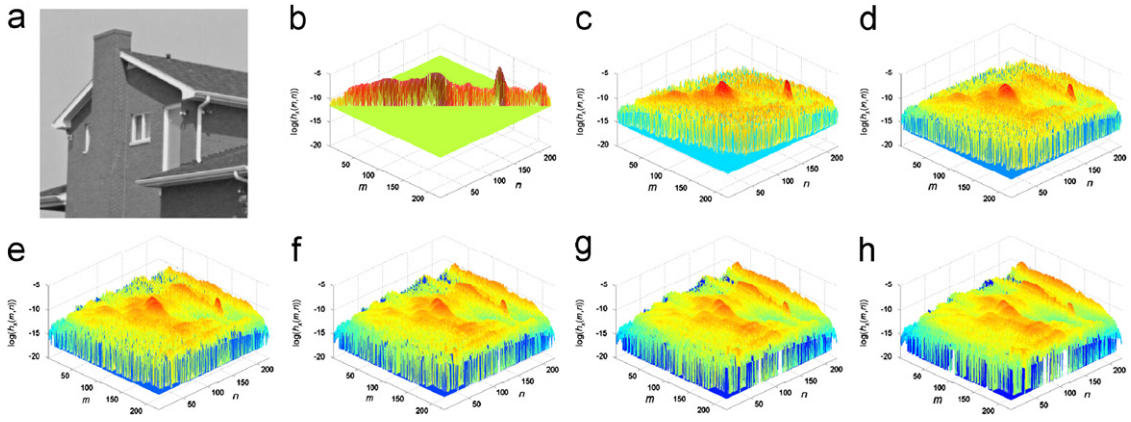

Fig. 1. The input *House* image (a) and its normalized 2D histograms according to Eq. (4) using neighbourhoods of size 1×1 (b), 3×3 (c), 5×5 (d), 7×7 (e), 9×9 (f), 11×11 (g), and 13×13 (f). For display purpose, $h_x(m,n)$ is shown in logarithmic scale.

where

$$P_t(m') = \sum_{i=1}^{m'} \sum_{j=1}^{L} h_t(i,j) = \sum_{i=1}^{m'} L\frac{1}{L^2} = \frac{m'}{L}. \quad (8)$$

In order to enhance the image, the grey-levels of the input image are transformed to the output grey-levels for a given output range of $[y_d,y_u]$ using the cumulative distribution functions $P_x(m)$ and $P_t(m')$. The input grey-level x_m is mapped to the output grey-level $y_{m'}$ by finding an index m' for a given index m according to

$$m' = \underset{i \in \{1,2,\ldots,L\}}{\operatorname{argmin}} \left|P_x(m) - P_t(i)\right|. \quad (9)$$

Using Eq. (9), each distinct grey-level of the input image $\mathbf{X}$ is transformed to a corresponding output grey-level to create an enhanced output image $\mathbf{Y}$. For ease of mathematical notation, the subscript w in $\mathbf{Y}_w$ is used to note that the output image is obtained using 2DHE with square $w \times w$ neighbourhood around each pixel is used in creating 2D histogram.

The resultant enhanced *House* images for different values of w are shown in the first row of Fig. 2 for $[y_d,y_u] = [0, 255]$ with the input to output grey-level data mappings shown in the second row of Fig. 2 and enhanced image histograms shown in the last row of Fig. 2. Fig. 2(b) shows the result of 2DHE when $w=1$ which is the same output with that of HE. Fig. 2 shows that when the contextual information is utilized 2DHE increases the brightness of the input image while keeping the high contrast between object regions when it is compared with the performance of HE shown in Fig. 2(b). Thus, the effect of 2DHE can be noticed when $w > 1$.

The proposed 2D histogram representation is a generalized version of HE. When 1×1 (only single pixel is considered without its neighbourhood) is utilized, the diagonal elements of 2D histogram as shown in Fig. 1(b) corresponds to 1D histogram of the input image. Thus, HE is a special case of the proposed algorithm with $w=1$.

2.2. Automatic parameter selection

2DHE is designed to improve visual impact by contrast enhancement without resulting in uncomfortable viewing. It depends on the parameter w. Different parameter settings result in different output images. One can fine tune the parameter w according to perceived contrast to create desired output. However, automatic parameter setting for which the output image has higher contrast with respect to the input image makes the algorithm to be applicable for general purpose contrast enhancement applications.

The parameter w has a finite feasible range. Thus, each different value of w from a finite set of possible values can be quantified using the output image. An output image is considered to have been enhanced over the input image if it enables the image details to be better perceived. The information content of the input image should be conserved in the output image. Considering these observations, the output image produced by the 2DHE is quantified according to a metric which combines discrete entropy together with measure of contrast.

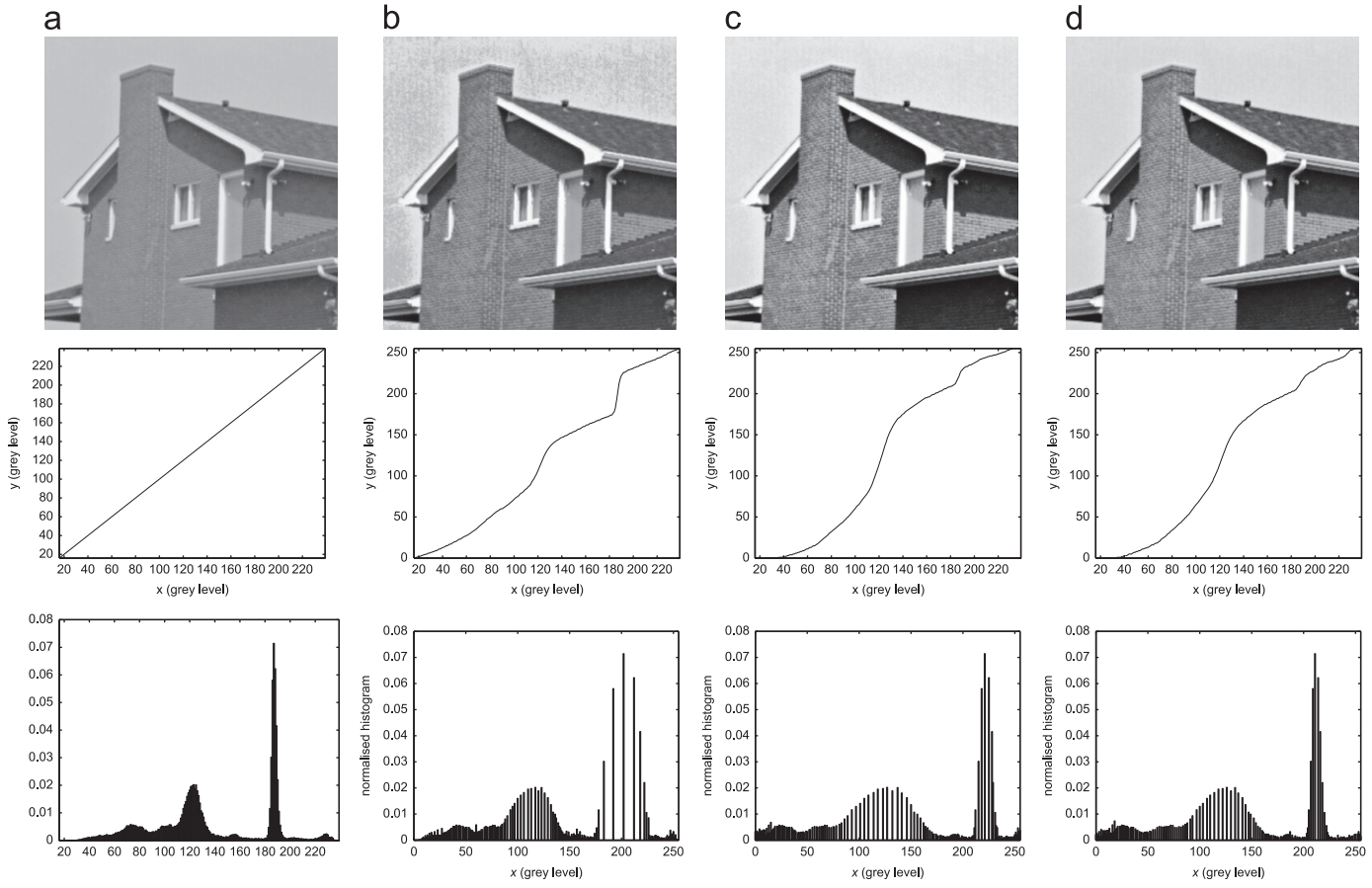

Fig. 2. Enhancing the input image shown in (a) using different size of local neighbourhood. The first, second, and third rows are grey scale images, input ($\mathcal{X}$) to output ($\mathcal{Y}$) grey-level data mapping, and 1D histogram of the corresponding grey-level image, respectively. (a) Input, (b) $w=1$, (c) $w=3$, (d) $w=5$.

The discrete entropy (DE) [16] of the input image $\mathbf{X}$ with K distinct grey-levels is

$$DE(\mathbf{X}) = -\sum_{k=1}^{K} p(x_k)\log p(x_k), \tag{10}$$

where $p(x_k)$ is the probability of pixel intensity x_k which is estimated from the normalized histogram. Similarly, the discrete entropy of the output image $\mathbf{Y}_w$ with L distinct grey-levels is defined as

$$DE(\mathbf{Y}_w) = -\sum_{l=1}^{L} p(y_l)\log p(y_l), \tag{11}$$

where $p(y_l)$ is the probability of pixel intensity y_l. A higher value of DE indicates the image has richer details. Using the metrics $DE(\mathbf{X})$ and $DE(\mathbf{Y}_w)$, the normalized discrete entropy ($DE_{\mathrm{N}}(\mathbf{X},\mathbf{Y}_w) \in [0,1]$) between input image $\mathbf{X}$ and output image $\mathbf{Y}_w$ is defined as

$$DE_{\mathrm{N}}(\mathbf{X},\mathbf{Y}_w) = \frac{1}{1+\dfrac{(\log(256)-DE(\mathbf{Y}_w))}{(\log(256)-DE(\mathbf{X}))}}, \tag{12}$$

where $\log(256)$ is the maximum value of entropy that can be achieved using 8-bits data representation. For $DE_{\mathrm{N}}(\mathbf{X},\mathbf{Y}_w) > 0.5$, the output image $\mathbf{Y}_w$ has higher discrete entropy than that of the input image $\mathbf{X}$, and vice versa. The higher the value of normalized discrete entropy, the better the enhancement is in terms of utilizing the dynamic range and providing better image details.

The edge based contrast measure (CM) is based on the observation that the human perception mechanisms are very sensitive to contours (or edges) [17]. The grey level corresponding to object frontiers is obtained by computing the average value of the pixel grey levels weighted by their edge values. The contrast $c(i,j)$ for a pixel of an image $\mathbf{X}$ located at (i,j) is thus defined as

$$c(i,j) = \frac{|x(i,j)-e(i,j)|}{|x(i,j)+e(i,j)|}, \tag{13}$$

where the mean edge grey level is

$$e(i,j) = \sum_{(k,l)\in\mathcal{N}(i,j)} g(k,l)x(k,l) \Big/ \sum_{(k,l)\in\mathcal{N}(i,j)} g(k,l), \tag{14}$$

$\mathcal{N}(i,j)$ is the set of all neighbouring pixels of pixel (i,j), and $g(k,l)$ is the edge value at pixel (k,l). Without loss of generality we employ 3×3 neighbourhood, and $g(k,l)$ is the magnitude of the image gradient estimated using the Sobel operators [5]. CM for image $\mathbf{X}$ is thus computed as the average contrast value, i.e.,

$$CM(\mathbf{X}) = \sum_{i=1}^{H}\sum_{j=1}^{W} c(i,j) \Big/ HW. \tag{15}$$

It is expected that for an output image $\mathbf{Y}_w$ of an input image $\mathbf{X}$, the contrast is improved when $CM(\mathbf{Y}_w) \geq CM(\mathbf{X})$. Using this observation, we define a new measure normalized edge based contrast measure CM_{N} between input image $\mathbf{X}$ and output image $\mathbf{Y}_w$ as follows:

$$CM_{\mathrm{N}}(\mathbf{X},\mathbf{Y}_w) = \frac{1}{1+\dfrac{(1-CM(\mathbf{Y}_w))}{(1-CM(\mathbf{X}))}}, \tag{16}$$

where $CM_{\mathrm{N}}(\mathbf{X},\mathbf{Y}_w) \in [0,1]$. When the output image $\mathbf{Y}_w$ has lower contrast than that of the input image $\mathbf{X}$, the corresponding $CM_{\mathrm{N}}(\mathbf{X},\mathbf{Y}_w)$ becomes $CM_{\mathrm{N}}(\mathbf{X},\mathbf{Y}_w) < 0.5$. $CM_{\mathrm{N}}(\mathbf{X},\mathbf{Y}_w) \geq 0.5$ corresponds to cases where the output image $\mathbf{Y}_w$ has higher contrast value than that of the input image $\mathbf{X}$.

By considering the finite range of w, the measures $DE_{\mathrm{N}}(\mathbf{X},\mathbf{Y}_w)$ and $CM_{\mathrm{N}}(\mathbf{X},\mathbf{Y}_w)$ between input image $\mathbf{X}$ and output image $\mathbf{Y}_w$ are first normalized into the interval of $[0,1]$ and are then combined under a single measure, referred to as discrete entropy and contrast measure ($DECM(\mathbf{X},\mathbf{Y}_w)$) using harmonic mean, i.e.,

$$DECM(\mathbf{X},\mathbf{Y}_w) = \frac{2}{\dfrac{1}{DE_{\mathrm{N}}(\mathbf{X},\mathbf{Y}_w)} + \dfrac{1}{CM_{\mathrm{N}}(\mathbf{X},\mathbf{Y}_w)}}, \tag{17}$$

where $DECM(\mathbf{X},\mathbf{Y}_w) \in [0,1]$ gives high values when the normalized discrete entropy and contrast measures are high, and vice versa. Thus, for a range of possible values of parameter w, the value of w (w_o) can be automatically selected according to the first local maximum value of $DECM(\mathbf{X},\mathbf{Y}_w)$ resulted from enhanced images with different realizations of w, i.e.,

$$w_o = \underset{\forall w\in[3,\min(H,W)/2]}{\text{arglocalmax}}\ DECM(\mathbf{X},\mathbf{Y}_w). \tag{18}$$

Although the range $[3,\min(H,W)/2]$ is large, the measure usually converges to local maximum for $w \leq 15$.

In the third row of Fig. 3 plots of metrics $DE_{\mathrm{N}}(\mathbf{X},\mathbf{Y}_w)$, $CM_{\mathrm{N}}(\mathbf{X},\mathbf{Y}_w)$, and $DECM(\mathbf{X},\mathbf{Y}_w)$ are shown for output images resulted from applying 2DHE on input images shown in the first row of Fig. 3 using variable window size parameter w. The second row of Fig. 3 shows the output images resulted from 2DHE using automatic window parameter selection according to Eq. (18). As can be easily noticed, 2DHE with automatic window size parameter w selection produces visually pleasing results.

2.3. Colour image enhancement

One approach to extend the grey-level contrast enhancement algorithm to colour images is to apply the algorithm to their luminance component only and preserve the chrominance components. Another is to multiply the chrominance values with the ratio of their input and output luminance values to preserve the hue. The former approach is employed in this paper where an input RGB image is transformed to CIE $L^*a^*b^*$ colour space [5] and the luminance component L^* is processed for contrast enhancement. The inverse transformation is then applied to obtain the contrast enhanced RGB image.

3. Experimental results

We used a dataset comprising standard test images from [18,19] to evaluate and compare the proposed algorithm with our implementations of HE [5], MWCVMHE [11], FHSABP [13], the weighted histogram approximation of HMF [14], and CEBGA [15]. All algorithms except HMF do not require parameter tuning. The parameter of HMF is set by maximizing its performance for a given input image in terms of visual quality and quantitative measures. For the proposed algorithm, automatic parameter selection is used. The test images show wide variations in terms of average image intensity and contrast. Thus they are suitable for measuring the strength of a contrast enhancement algorithm under different circumstances.

3.1. Quantitative measures

An output image is considered to have been enhanced over the input image if it enables the image details to be better perceived. An assessment of image enhancement is not an easy task as an improved perception is difficult to quantify. Nevertheless, in practice it is desirable to have both quantitative and subjective assessments. It is therefore necessary to establish a basis which defines a good measure of enhancement. In order to quantify contrast enhancement between input image $\mathbf{X}$ and output image $\mathbf{Y}$, we use normalized discrete entropy $DE_{\mathrm{N}}(\mathbf{X},\mathbf{Y})$ defined in

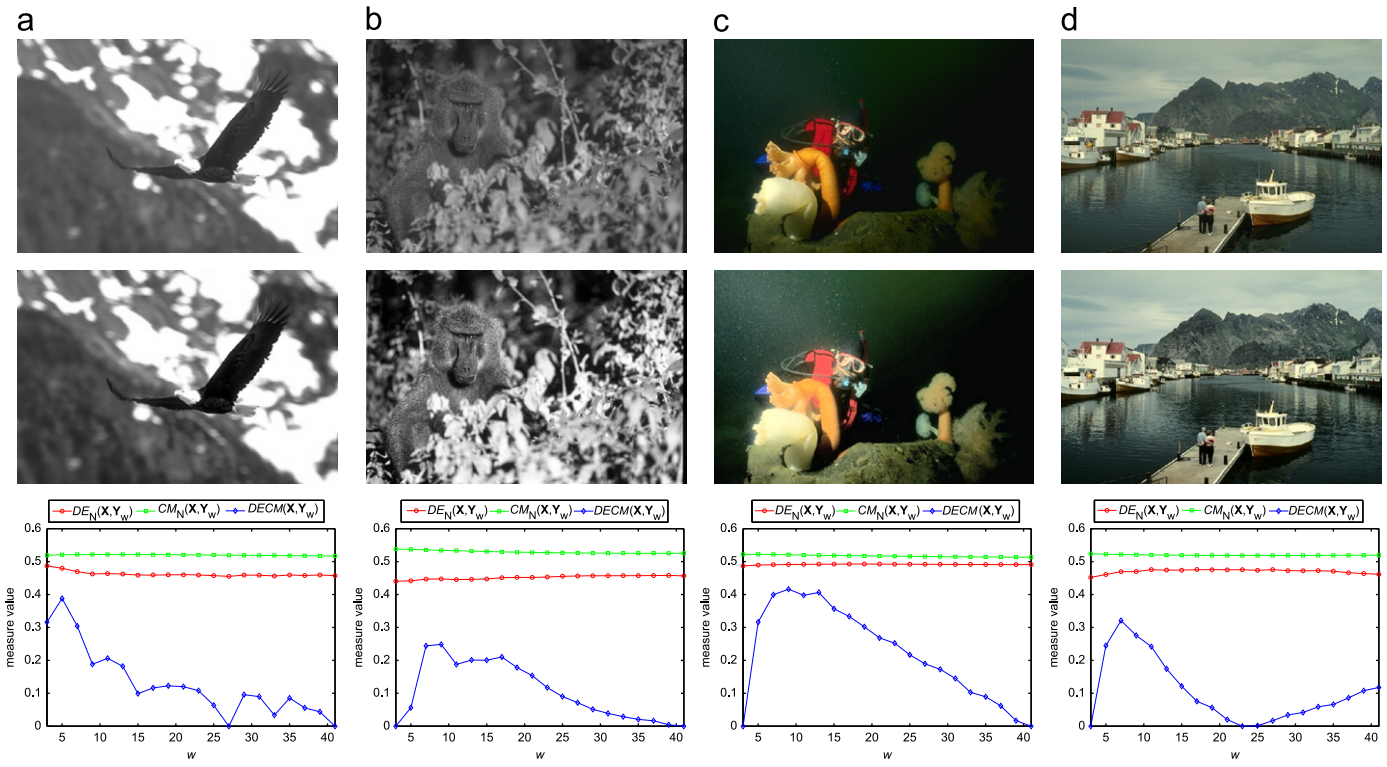

Fig. 3. Enhancing the input images shown in the first row by automatically selecting window parameter w according to Eq. (18) which utilizes metrics shown in the third row to produce the output images shown in the second row. (a) $w_o = 5$, (b) $w_o = 9$, (c) $w_o = 9$, (d) $w_o = 7$.

Eq. (12) and normalized edge based contrast measure $CM_N(\mathbf{X},\mathbf{Y})$ defined in Eq. (16).

For a consumer electronics application brightness preservation may be used as pre-condition in contrast enhancement process. Thus, one needs to quantify the brightness preservation. We adopt absolute mean brightness error (*AMBE*) [10] which is the absolute difference between the mean values of input image **X** and output image **Y** to define the normalized absolute mean brightness error ($AMBE_N \in [0,1]$), i.e.,

$$AMBE_N(\mathbf{X},\mathbf{Y}) = \frac{1}{1+|MB(\mathbf{X})-MB(\mathbf{Y})|}, \tag{19}$$

where $MB(\mathbf{X})$ and $MB(\mathbf{Y})$ are the average values of **X** and **Y**, respectively. The higher the value of $AMBE_N$, the better is the brightness preservation, and vice versa.

3.2. Qualitative assessment

3.2.1. Grey-scale images

Some example contrast enhancement results and corresponding input to output grey-level mapping functions resulted from the different algorithms for grey-scale images are shown in Figs. 4–7.

The input (original) *Plane* image [18] in Fig. 4(a) shows a low-contrast image comprising light and dark regions corresponding to ground, plane and shadow. HE has darken the image considerably to increase the contrast between regions. This is verified by the mapping function in Fig. 4(h) which shows that the input grey-level range [3, 150] is mapped to output grey-level range [0, 12]. Although HE has increased the contrast between different regions of the input image, it considerably reduces the contrast within each region of the image. The entire plane is mapped to darker grey-levels, and thus most of its texture is not identifiable. MWCVMHE produces visually pleasing output image. This is because applying multi-histogram equalization reduces the over darkening effect of HE. However, one can easily notice that regions belonging to ground have low-contrast which makes it difficult to see the ground texture. FHSABP produces a brighter image which has better visual quality and contrast than the result of HE. The mapping function of FHSABP follows a similar shape as that of HE, but it maps the range [3, 150] to [0, 69]. Thus, it is also easier to identify the texture on the plane. Like HE, HMF finds a target histogram which is the minimum distance between input histogram and uniformly distributed histogram. It thus produces a similar shaped mapping function as that of HE. However, it maps [3, 150] to [0, 16] which results in a slightly brighter output image when it is compared with the result of HE. Due to the image details not being sharp, CEBGA can only change the overall brightness of the image. This is verified by the mapping function which is almost parallel to the no-change mapping. CEBGA maps input grey-level range [3, 150] to output grey-level range [1, 159] which results in almost no change in the output image, except for a slight increased in contrast. The contextual information in the image is considered when producing the 2D histogram, which makes it possible for the proposed algorithm to model the intensity values of ground, plane and shadow regions. Input grey-level values are assigned to output grey-level values according to the contextual information extracted from input image. The input grey-level range [3, 150] is mapped to output grey-level range [0, 90]. Thus, 2DHE improves the overall contrast while preserving the image details. In its output image, it is easy to identify the texture of the ground as well as the plane.

The input *Tank* image [18] in Fig. 5(a) has an average brightness value of 132. HE and FHSABP produce similar output images and similar mapping functions as shown in Fig. 5(h). This is because the average brightness value is very near to 127. The contrast between the tank and its surrounding is significantly increased. However, the details in the darker area of the tank body are barely noticeable. The output of MWCVMHE has higher

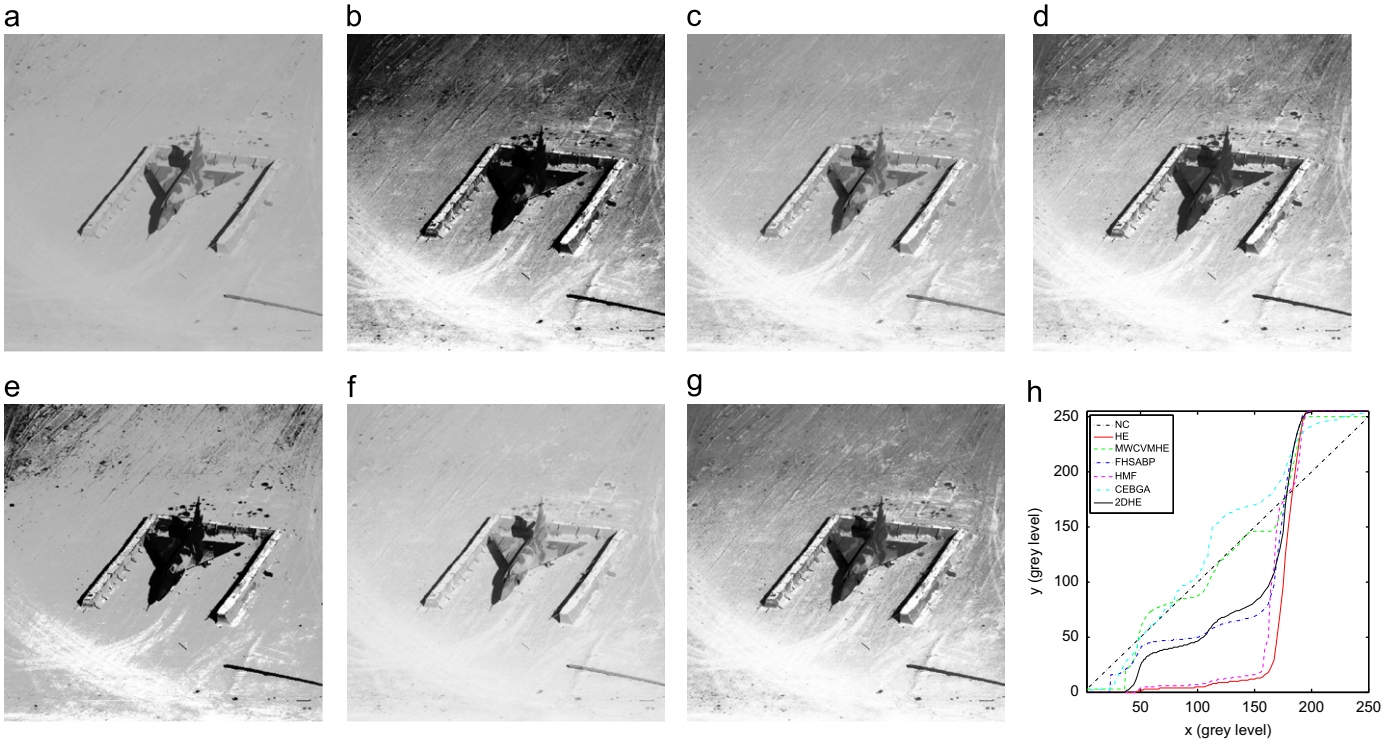

Fig. 4. Contrast enhancement results for image *Plane*. (a) Original image. Enhanced images obtained using: (b) HE; (c) MWCVMHE; (d) FHSABP; (e) HMF; (f) CEBGA; and (g) 2DHE. Input to output grey-level mapping functions of enhanced grey-scale images are shown in (h) where "NC" refers to no-change mapping.

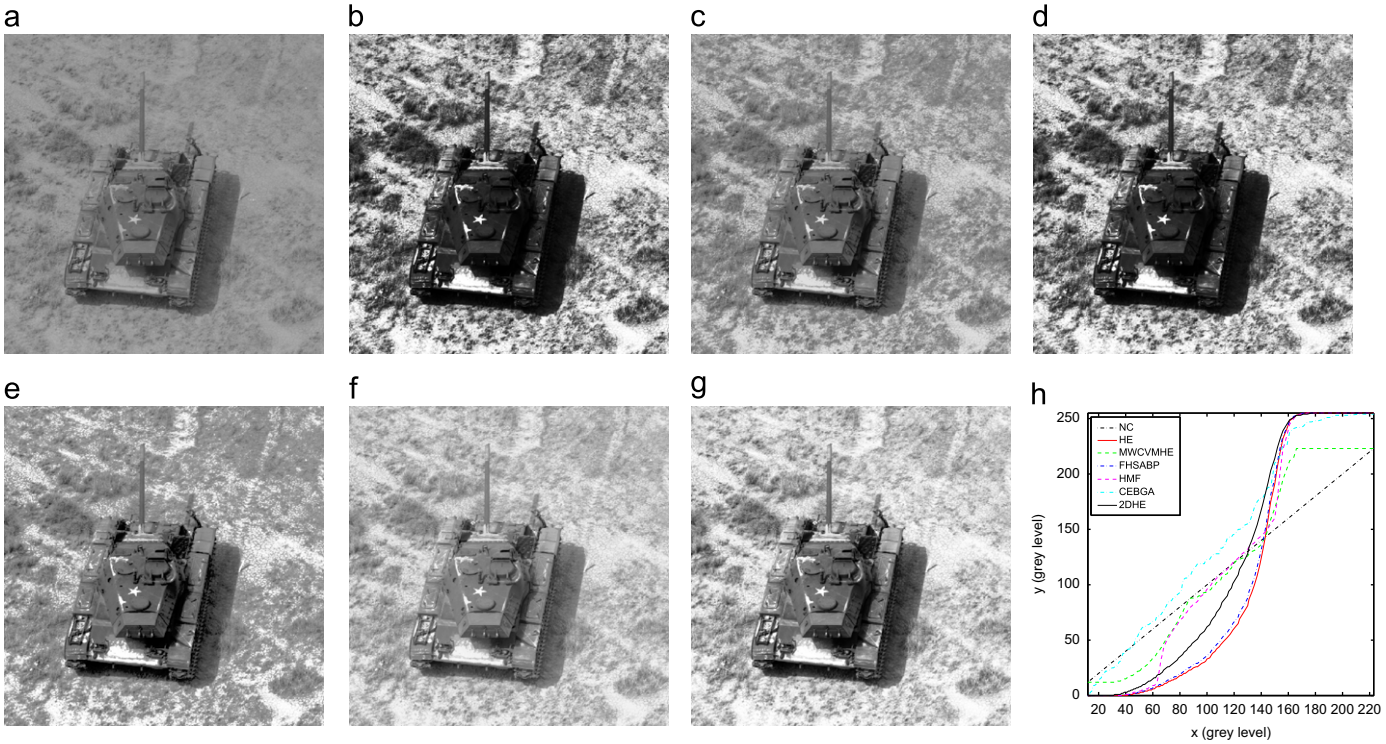

Fig. 5. Contrast enhancement results for image *Tank*. (a) Original image. Enhanced images obtained using: (b) HE; (c) MWCVMHE; (d) FHSABP; (e) HMF; (f) CEBGA; and (g) 2DHE. Input to output grey-level mapping functions of enhanced grey-scale images are shown in (h) where "NC" refers to no-change mapping.

contrast than that of the input image, however, the overall contrast can be further improved by using the whole dynamic range. The output of HMF is visually pleasing and the contrast between the tank and its surrounding is high enough to reveal details on both the tank and its surrounding. However, when the ground is closely observed, the details of the tank track created by its palettes are lost in the enhanced image. CEBGA produces a higher contrast image but bright when it is compared with the input image. The output image of the 2DHE has high enough contrast to reveal the different objects and their details in the

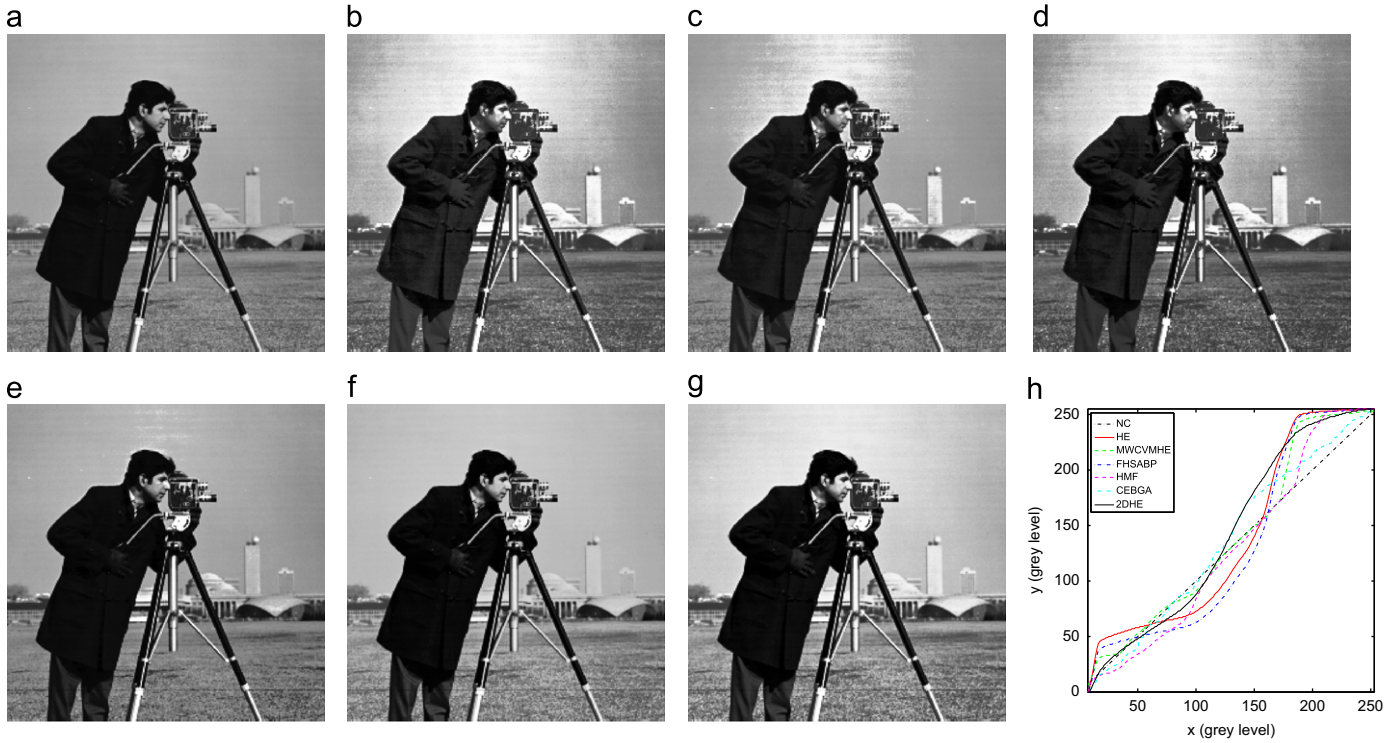

Fig. 6. Contrast enhancement results for image *Cameraman*. (a) Original image. Enhanced images obtained using: (b) HE; (c) MWCVMHE; (d) FHSABP; (e) HMF; (f) CEBGA; and (g) 2DHE. Input to output grey-level mapping functions of enhanced grey-scale images are shown in (h) where "NC" refers to no-change mapping.

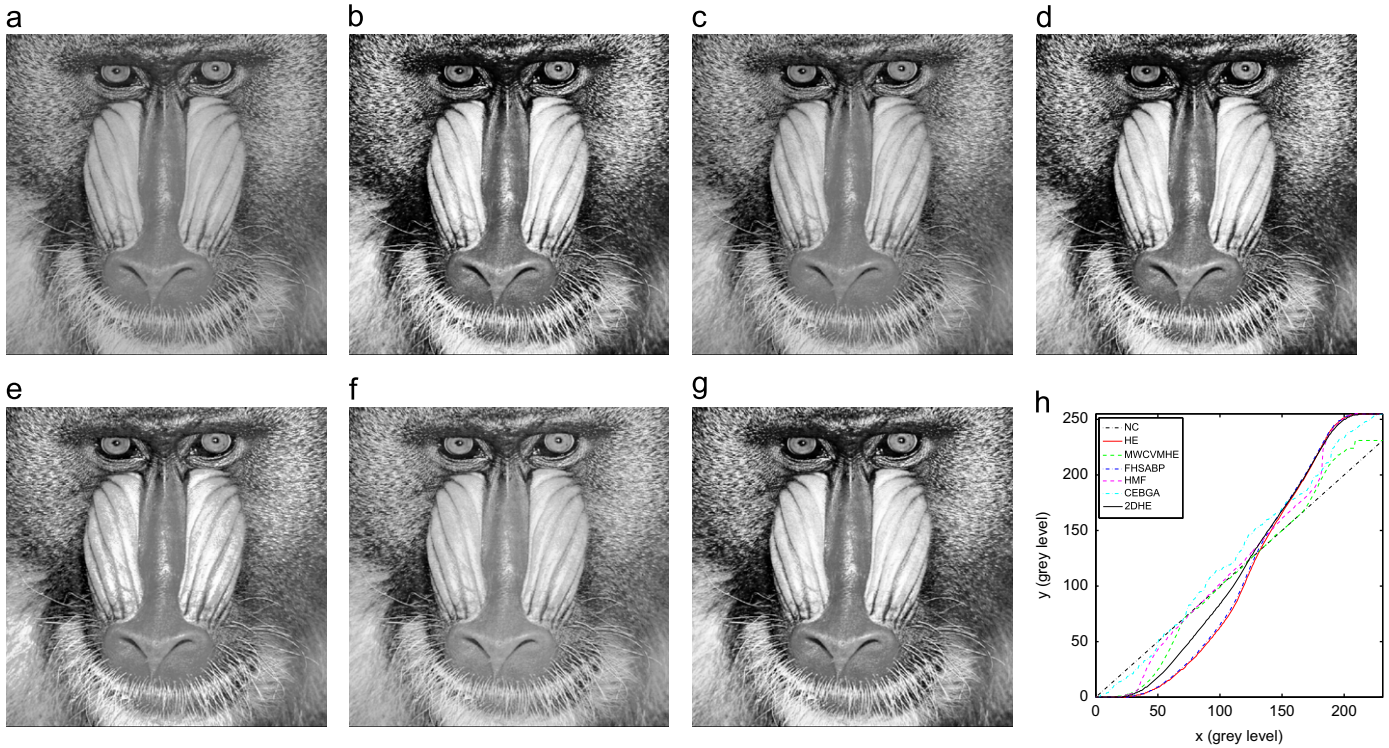

Fig. 7. Contrast enhancement results for image *Baboon*. (a) Original image. Enhanced images obtained using: (b) HE; (c) MWCVMHE; (d) FHSABP; (e) HMF; (f) CEBGA; and (g) 2DHE. Input to output grey-level mapping functions of enhanced grey-scale images are shown in (h) where "NC" refers to no-change mapping.

image. The tank and its details, tank tracks, bushes and other details on the ground can be easily identified.

The input *Cameraman* image shown in Fig. 6(a) has very dark and bright regions. The dark colour of the cameraman's coat makes it difficult to identify its details, e.g., buttons and front pocket. Behind the cameraman are the light coloured sky and buildings in shade varying between dark and light. The input image has a dynamic range of [7, 253] and has average brightness

value of 119. The output images of HE, MWCVMHE and FHSABP, and their mapping functions in Fig. 6(h) reveal that they produce very similar results. In both enhanced images, it is easy to identify the details of the coat. However, the deformations caused by mapping on the sky and cameraman's face degrade the visual quality. HMF improves the contrast significantly with slight deformations on the sky. The deformations on the sky region are caused by the sharp change in its mapping function toward higher grey levels. Furthermore, it is hard to identify the details on the coat. Due to the high contrast between the coat and the background, and utilization of full dynamic range in input image, CEBGA achieves slight enhancement which is verified by its mapping function. 2DHE produces increased contrast while keeping the details on the different regions in the enhanced image. The details of the coat can be easily identified, and the enhanced image is free of the deformations in the results of HE, FHSABP and HMF.

The input *Baboon* image shown in Fig. 7(a) has very rich texture content and has an average brightness value of 129. HE and FHSABP produces almost the same results which are verified by their mapping function in Fig. 7(h). MWCVMHE, HMF and CEBGA generate similar output images. However, the contrast of these images is not as high as those of HE and FHSABP. 2DHE also performs similarly to HE and FHSABP with slightly higher brightness mapping for lower values of the input grey-levels. However, when the output image of the proposed algorithm is compared with those of HE and FHSABP, it provides clearer details especially around the dark region left of the baboon's nose.

3.2.2. Colour images

Some example contrast enhancement results and corresponding input to output grey-level mapping functions resulted from the different algorithms for colour images are shown in Figs. 8–11.

Fig. 8. Contrast enhancement results for image *Cessna*. (a) Original image. Enhanced images obtained using: (b) HE; (c) MWCVMHE; (d) FHSABP; (e) HMF; (f) CEBGA; and (g) 2DHE. Input to output grey-level mapping functions of enhanced grey-scale images are shown in (h) where "NC" refers to no-change mapping. (For interpretation of the references to color in this figure caption, the reader is referred to the web version of this article.)

Fig. 9. Contrast enhancement results for image *Lighthouse*. (a) Original image. Enhanced images obtained using: (b) HE; (c) MWCVMHE; (d) FHSABP; (e) HMF; (f) CEBGA; and (g) 2DHE. Input to output grey-level mapping functions of enhanced grey-scale images are shown in (h) where "NC" refers to no-change mapping. (For interpretation of the references to color in this figure caption, the reader is referred to the web version of this article.)

Fig. 10. Contrast enhancement results for image *Beach*. (a) Original image. Enhanced images obtained using: (b) HE; (c) MWCVMHE; (d) FHSABP; (e) HMF; (f) CEBGA; and (g) 2DHE. Input to output grey-level mapping functions of enhanced grey-scale images are shown in (h) where "NC" refers to no-change mapping. (For interpretation of the references to color in this figure caption, the reader is referred to the web version of this article.)

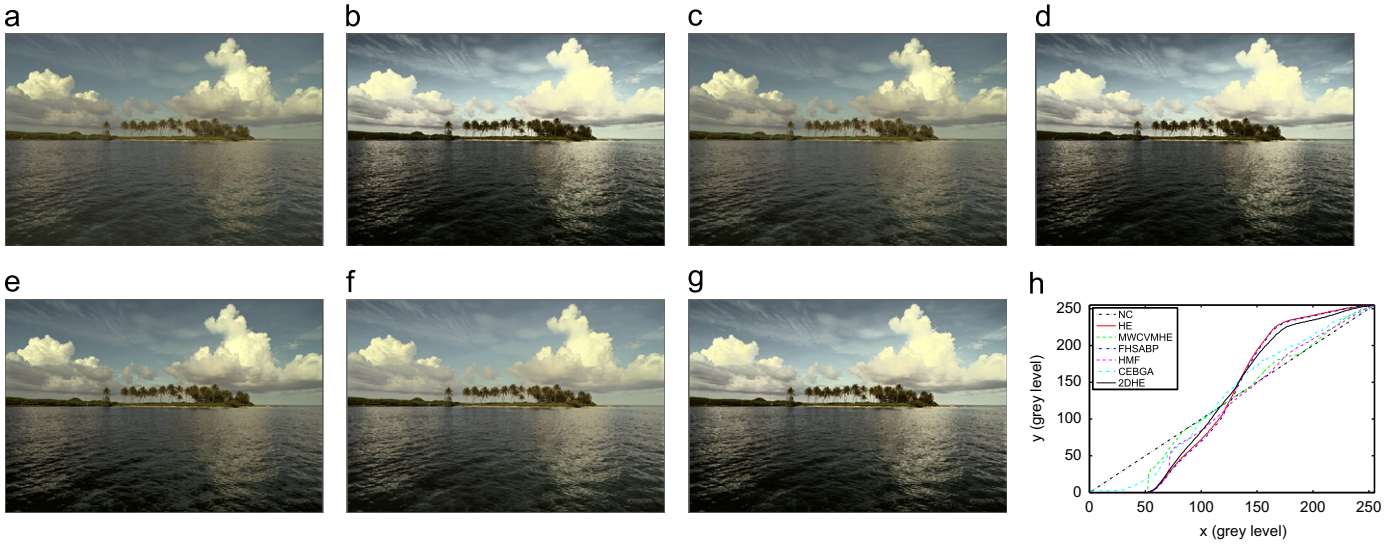

Fig. 11. Contrast enhancement results for image *Island*. (a) Original image. Enhanced images obtained using: (b) HE; (c) MWCVMHE; (d) FHSABP; (e) HMF; (f) CEBGA; and (g) 2DHE. Input to output grey-level mapping functions of enhanced grey-scale images are shown in (h) where "NC" refers to no-change mapping. (For interpretation of the references to color in this figure caption, the reader is referred to the web version of this article.)

The input image *Cessna* in Fig. 8(a) shows a plane on a grass field against a background of sky. Due to the bright white sky with a faint orange tint while the rest of the image (i.e., regions below the plane) is relatively dark, it is difficult to discriminate the details on the plane and its surrounding. HE, FHSABP and HMF generate similar output images with high image degradations. This is especially so in the sky region where the original orange tint has been separated into noticeable layers of coloured regions ranging from dark orange to light grey. The various details in the image are not as clear as in the input image due to the darkening of the image in the case of the results of HE and HMF, and the lightening of the result of FHSABP. Fig. 8(h) shows that except for the differences in terms of brightness level the input to output grey-level mapping functions of HE, FHSABP and HMF are very similar, i.e., similar shaped curves parallel to one another. As can be noticed from mapping function of MWCVMHE, it makes almost no change between the input and output images. CEBGA generates a slightly improved output image in the area below the plane with no degradations in the sky. Its mapping function is similar to the no-change mapping function except for the mid-grey level range. 2DHE, on the other hand, provides an output image with no image degradations in the sky, and the details on the plane are clearly visible. This is because of its input to output grey-level mapping function shows both the low and mid-to-high grey level ranges have been stretched with varying degree but not too excessive to cause image degradations.

For the input *Lighthouse* image shown in Fig. 9(a), the over enhancement provided by HE and FHSABP darken some areas of the cliff, sea and sky. There is loss of details in the darkened regions. Fig. 9(h) shows that this darkening effect is caused by both mapping functions stretching the low to mid-grey level range much more than the mid-grey to high grey level range. Since the mapping functions of MWCVMHE, HMF and CEBGA are both similar to the no-change mapping they generate similar

results with a slight increase in contrast. On the other hand, 2DHE increases both the contrast and the average brightness to improve the overall image quality. The details in the image are also clearer.

For the input *Beach* image as shown in Fig. 10(a), HE and HMF cause the couple and the distant hill to be too dark, thus their details are not visible. The darkening are verified by the mapping of a greater range of low-to-high grey levels in the input image to the low grey levels in the output image as shown in Fig. 10(h). MWCVMHE, FHSABP, CEBGA and 2DHE increase the overall contrast considerably by making the colours in the image richer while maintaining high visual quality which enables image details to be identified.

For the input *Island* image as shown in Fig. 11(a), MWCVMHE, HMF and CEBGA produce output images which have slightly improved contrast with respect to the input image. This can also be verified from the mapping functions shown in Fig. 11(h). HE, FHSABP and 2DHE provide contrast enhancement in terms of richer colours and increased contrast, while retaining the details and visual quality.

3.2.3. Visual assessment score

In order to assign a visual assessment score to each algorithm for each enhanced image, subjective perceived quality tests are performed by a group of 15 subjects on the results of the six contrast enhancement algorithm for the eight test images. For each test on a test image, a subject is shown seven images at the same time: the original test image (placed in the centre of view) and the output images processed by six algorithms (randomly placed around the original test image). The subject is then asked to score the quality of the processed image by assigning one of the six numeric scores (0, 1, 2, 3, 4 and 5), where score "0" is for very bad and annoying enhancement (the image quality is totally distorted), score "3" is for no noticeable enhancement (natural and similar to the original image), score "5" is for significant enhancement without annoying distortion (looks natural across the overall image), and other values are selected according to the perceived image quality.

The mean opinion scores (MOSs) and the corresponding standard deviations of the visual assessment are shown in Table 1. The MOS support the qualitative assessments in Section 3.2. For each test image, the standard deviations of MOS of different algorithms are similar, which indicate the uncertainty of each subject in scoring is similar. Table 1 also shows that only 2DHE always improve the image quality since all of their MOS are greater than 3 (where score "3" indicates natural and similar to the original image).

3.3. Quantitative assessment

The visual assessments are supplemented by the computed quantitative measures tabulated in Tables 2–4 for measures $AMBE_N$, DE_N and CM_N, respectively. For colour images, the measures are calculated on their luminance channel only.

The average $AMBE_N$ in Table 2 values show that FHSABP outperforms all other algorithms in brightness preservation except. This is an expected result since FHSABP employs an optimization algorithm with a constraint of keeping the mean brightness values of input and output image the same. However, preserving the mean brightness does not always preserve the

Table 2
Quantitative measurement results as $AMBE_N$.

Image	HE	MWCVMHE	FHSABP	HMF	CEBGA	2DHE
Plane	0.0260	0.0824	0.1246	0.2328	0.0330	0.3269
Tank	0.4928	0.1039	0.2140	0.0661	0.0239	0.0360
Cameraman	0.0944	0.1471	0.5470	0.2601	0.0782	0.0473
Baboon	0.3618	0.4936	0.7338	0.0938	0.0564	0.1276
Cessna	0.0197	0.2926	0.2308	0.0392	0.2225	0.5973
Lighthouse	0.1141	0.7862	0.5283	0.1587	0.4376	0.0973
Beach	0.0198	0.1603	0.6743	0.0467	0.0371	0.0245
Island	0.2495	0.5470	0.5625	0.0932	0.1524	0.1873
Average	0.1723	0.3266	0.4519	0.1238	0.1301	0.1805

Table 3
Quantitative measurement results as DE_N.

Image	HE	MWCVMHE	FHSABP	HMF	CEBGA	2DHE
Plane	0.4920	0.4909	0.4973	0.4935	0.4975	0.4990
Tank	0.4880	0.4867	0.4895	0.4945	0.4525	0.4950
Cameraman	0.4458	0.4516	0.4432	0.4585	0.3876	0.4812
Baboon	0.4572	0.4630	0.4588	0.4785	0.3197	0.4802
Cessna	0.4623	0.4690	0.4558	0.4522	0.4560	0.4815
Lighthouse	0.4502	0.4597	0.4538	0.4847	0.3625	0.4866
Beach	0.4528	0.4630	0.4501	0.4619	0.4389	0.4767
Island	0.4532	0.4573	0.4517	0.4843	0.3787	0.4670
Average	0.4627	0.4677	0.4625	0.4760	0.4117	0.4830

Table 4
Quantitative measurement results as CM_N.

Image	HE	MWCVMHE	FHSABP	HMF	CEBGA	2DHE
Plane	0.5540	0.5138	0.5268	0.5299	0.5050	0.5264
Tank	0.5556	0.5197	0.5524	0.5296	0.5112	0.5351
Cameraman	0.5128	0.5060	0.5165	0.5071	0.5099	0.5158
Baboon	0.5422	0.5096	0.5408	0.5103	0.5031	0.5266
Cessna	0.5220	0.5040	0.4975	0.5064	0.5067	0.5103
Lighthouse	0.5348	0.5078	0.5310	0.5103	0.5049	0.5192
Beach	0.5305	0.5061	0.5116	0.5191	0.5097	0.5164
Island	0.5256	0.5072	0.5261	0.5189	0.5124	0.5234
Average	0.5347	0.5093	0.5253	0.5164	0.5079	0.5217

Table 1
Subjective quality test scores as mean opinion score (MOS).

Image	HE	MWCVMHE	FHSABP	HMF	CEBGA	2DHE
Plane	1.3 ± 1.1	3.5 ± 0.5	2.1 ± 0.3	0.3 ± 0.4	3.1 ± 0.9	4.5 ± 0.5
Tank	4.1 ± 0.9	3.1 ± 0.9	4.2 ± 0.8	4.1 ± 0.8	3.3 ± 0.6	4.3 ± 0.7
Cameraman	2.1 ± 1.1	2.3 ± 1.0	2.1 ± 0.9	3.2 ± 0.7	3.5 ± 0.6	3.8 ± 0.6
Baboon	4.6 ± 0.5	3.1 ± 0.2	4.5 ± 0.5	3.2 ± 1.1	3.2 ± 0.9	4.5 ± 0.3
Cessna	0.7 ± 0.8	2.5 ± 1.1	0.9 ± 1.1	0.7 ± 0.9	3.7 ± 1.0	3.9 ± 1.2
Lighthouse	4.5 ± 0.7	2.1 ± 0.8	4.5 ± 0.6	2.9 ± 0.7	2.9 ± 0.5	4.4 ± 0.3
Beach	2.7 ± 1.2	3.6 ± 1.3	3.3 ± 1.2	1.1 ± 1.2	3.8 ± 0.7	3.5 ± 1.0
Island	4.3 ± 1.3	2.4 ± 1.1	4.4 ± 1.2	3.1 ± 1.3	3.3 ± 0.9	4.4 ± 0.9

natural look of an image or increase the overall contrast. For example although FHSABP provides the best $AMBE_N$ value of 0.5470 for the *Cameraman* image, its output image as shown in Fig. 6(d) is worse than the input image in terms of visual quality and contrast. Conversely, although the proposed algorithm performs worse than FHSABP in terms of average $AMBE_N$, unlike FHSABP the visual assessment scores of all of its enhanced images are above 3 which means it produces visually pleasing images with respect to input images.

Table 5
Average quantitative measurement results as $AMBE_N$, DE_N and CM_N on 300 test images from Berkeley image dataset [20].

Method	$AMBE_N$	DE_N	CM_N
HE	0.1034	0.4496	0.5253
MWCVMHE	0.5014	0.4651	0.5064
FHSABP	0.5468	0.4531	0.5231
HMF	0.1182	0.4572	0.5141
CEBGA	0.1746	0.3610	0.5103
2DHE	0.2052	0.4822	0.5263

The DE_N values in Table 3 show that the proposed algorithm outperforms all the other algorithms. Although one would expect HE to give a higher entropy as its results have a more uniform histogram distribution, HE groups bins and this decreases the DE_N value. Since MWCVMHE and FHSABP behave similarly to HE, their DE_N values are similar to HE. Since HMF also preserves the overall entropy of an image, its DE_N values are thus high. CEBGA provides the lowest DE_N value because it generally maps consecutive grey values of the input image to the same grey values in the output image, which reduces the overall entropy of the output image. The high value of DE_N, which is generally very close to that of the input image, shows that the proposed algorithm is successful in

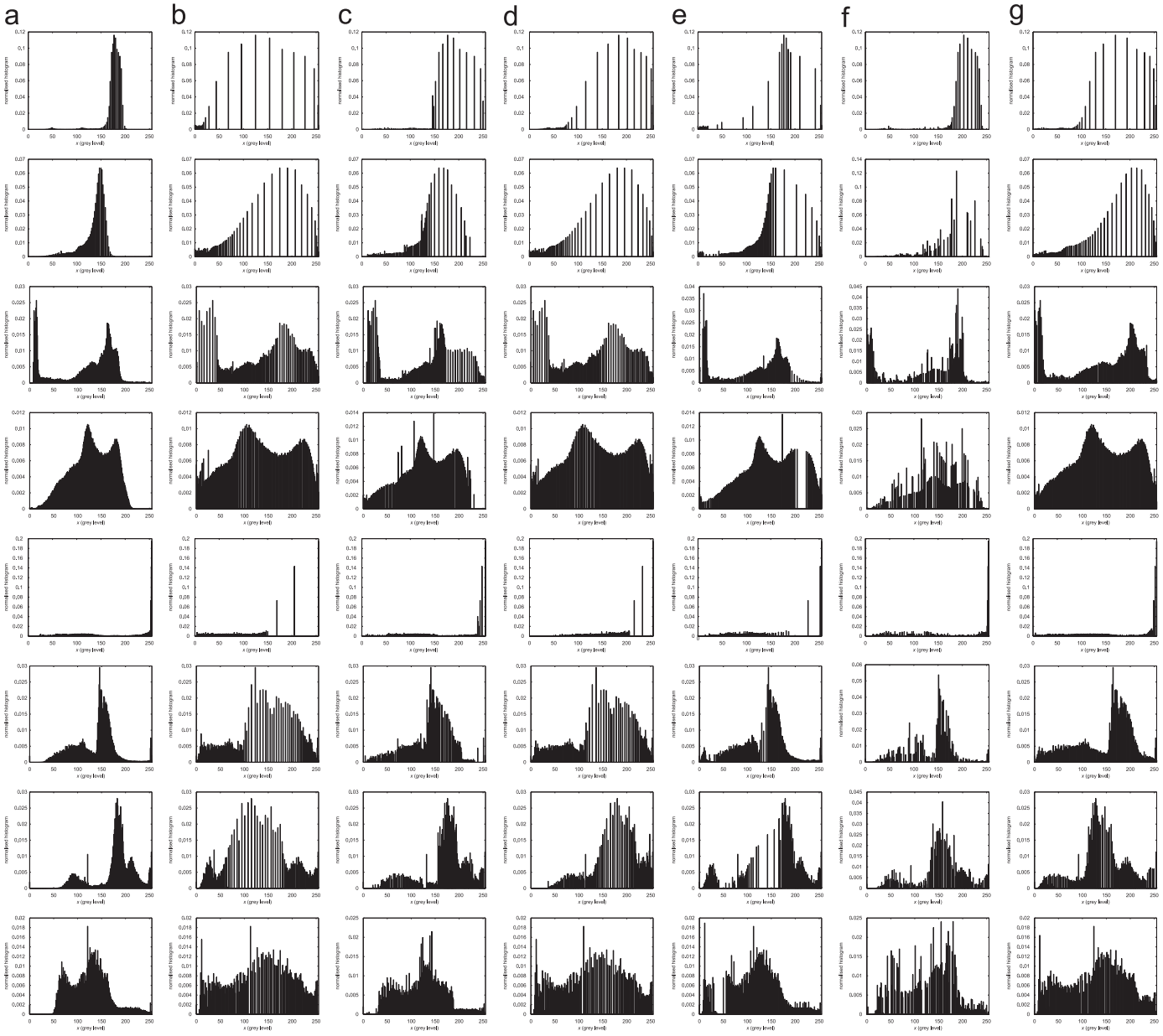

Fig. 12. Histograms of input images (a) and enhanced images obtained using: (b) HE; (c) MWCVMHE; (d) FHSABP; (e) HMF; (f) CEBGA; and (g) 2DHE. From top to bottom each row shows the results for *Plane*, *Tank*, *Cameraman*, *Baboon*, *Cessna*, *Lighthouse*, *Beach* and *Island* images, respectively. For colour images, the histograms are shown for luminance component (L^* component). (For interpretation of the references to color in this figure caption, the reader is referred to the web version of this article.)

preserving the contextual information while improving the visual quality.

The CM_N values in Table 4 show that HE achieves the best performance. FHSABP and the proposed algorithm produces DE_N values that are larger than those of MWCVMHE, HMF and CEBGA, but lower than that of HE. They thus achieve the second best in performance according to this quantitative measure.

In order to evaluate the performance of the six algorithms for a wide range of images, they are applied to 300 test images from Berkeley image dataset [20]. The average measurement values of $AMBE_N$, DE_N and CM_N are reported in Table 5. Similar to the above presented results, FHSABP overcomes the other algorithms in terms of the average $AMBE_N$ value. Meanwhile, 2DHE achieves the best in terms of average DE_N and CM_N values. Thus, 2DHE achieves the best contrast enhancement due to the largest value of CM_N meanwhile it protects the content of the image better than the other algorithms considered in this paper as it produces the largest value of DE_N.

Table 6
Kullback–Leibler (KL) distances between the grey-level distributions of the processed output images resulted from different algorithms and uniform distribution.

Image	HE	MWCVMHE	FHSABP	HMF	CEBGA	2DHE
Plane	4.13	4.14	4.04	4.10	4.04	4.01
Tank	2.63	2.64	2.61	2.56	3.03	2.55
Cameraman	1.23	1.20	1.24	1.17	1.56	1.07
Baboon	0.76	0.74	0.76	0.70	1.37	0.69
Cessna	2.27	2.21	2.33	2.37	2.33	2.11
Lighthouse	1.22	1.17	1.20	1.06	1.75	1.06
Beach	1.41	1.35	1.42	1.36	1.49	1.28
Island	0.94	0.92	0.94	0.83	1.27	0.89

3.3.1. Assessing histogram equalization capability

Histogram equalization refers to processing input image to utilize the dynamic range efficiently by mapping an input into output image such that there is equal number of pixels at each grey-level in output. Thus, it is expected that the equalized output image has flattened grey-level distribution. However, it should be noted that the process should not change the overall shape of the input histogram to protect the image content.

In order to quantitatively measure how flattened the output grey-level distribution is Kullback–Leibler (KL) distance between the distribution of the processed output image ($p(y_k)$) and uniform distribution ($q(y_k)$) is used. The KL-distance is a natural distance function from a "true" probability distribution, $p(y_k)$, to a "target" probability distribution, $q(y_k)$, i.e.,

$$KL(p,q)=\sum_{\forall k} p(y_k)\log_2\left(\frac{p(y_k)}{q(y_k)}\right). \tag{20}$$

The lower the value of KL, the better the histogram equalization is.

In Fig. 12, the input and output histograms resulted from different algorithms are shown for the test images. The corresponding KL-distances are reported in Table 6. The results show that 2DHE preserves the shape of the histogram while it flattens it. According to the reported KL-distances, the best histogram equalization is achieved by 2DHE.

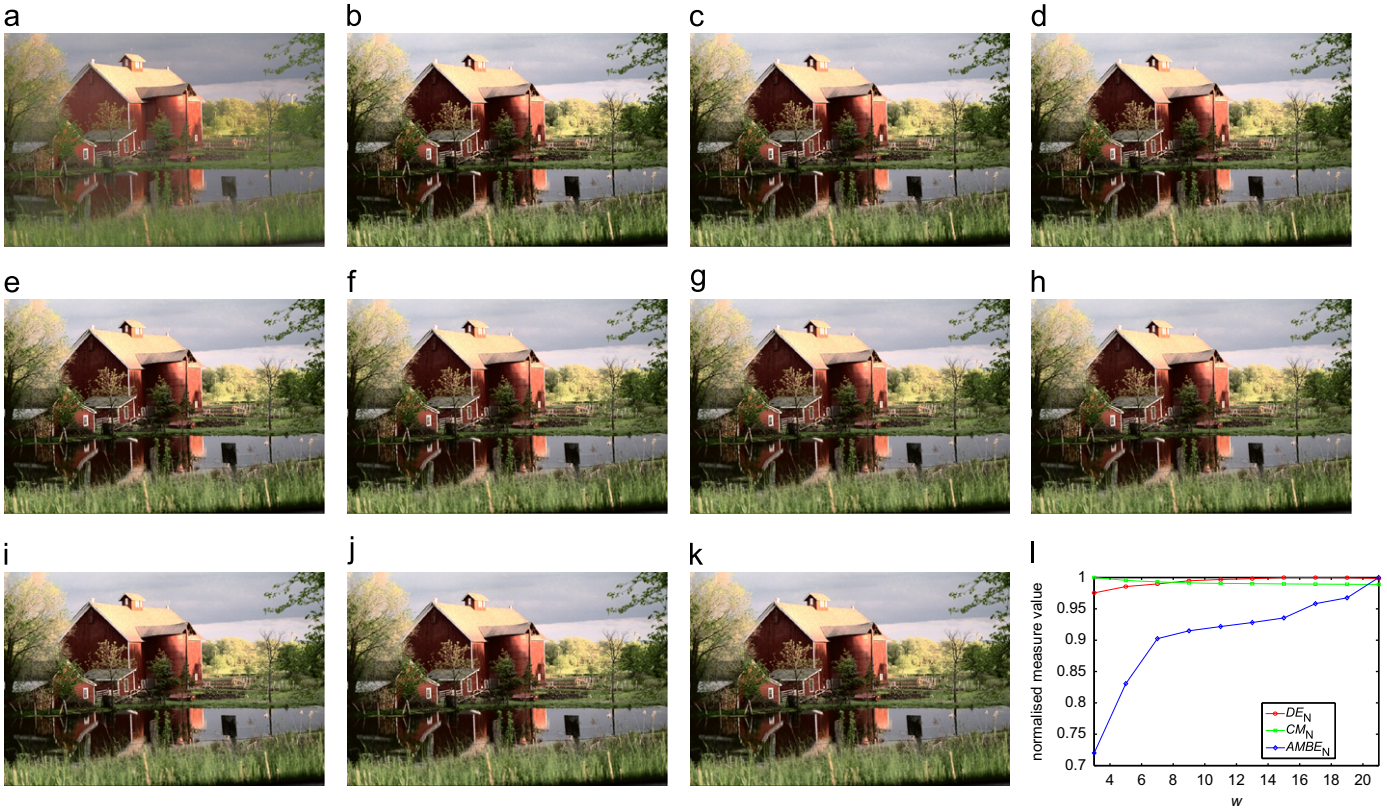

Fig. 13. (b–k) Results of the proposed algorithm on an input image (a) from Kodak dataset for different values of spatial neighbourhood parameter w. (l) The average quantitative measurement results of the enhanced images of 24 test images from Kodak dataset using the proposed algorithm for different values of local neighbour support parameter w. For display purpose all measures are normalized to $[0,1]$ by dividing each measure with the maximum measure. (a) Input, (b) $w=3$, (c) $w=5$, (d) $w=7$, (e) $w=9$, (f) $w=11$, (g) $w=13$, (h) $w=15$, (i) $w=17$, (j) $w=19$, (k) $w=21$ and (l).

3.4. The effect of spatial neighbourhood support

The parameter w which is used to define a square $w \times w$ spatial support of the neighbourhood around each pixel is the only tuning parameter of the proposed algorithm. The results presented in Sections 3.2 and 3.3 are for automatic parameter selection. Although automated parameter selection produces satisfactory results, one can further improve the output image by varying w. The higher the value of w, the more contextual information is utilized in the enhancement process. However, it should be noted that when the value of w gets larger, the contextual information around each pixel approaches the global contextual information of the image.

To demonstrate the effects of varying the size of the spatial neighbourhood support, 24 test images from Kodak dataset [19] are enhanced using the proposed algorithm for different values of w. The average of resulting quantitative measures is shown in Fig. 13(l), where for display purpose all measures are normalized to $[0,1]$ by dividing each measure with the maximum measure obtained. Samples of enhanced images for varying values of w are shown in Fig. 13(b)–(k) for a sample image from the Kodak dataset. It is clear that different performance results can be achieved by varying the spatial neighbourhood size.

The plots for $AMBE_N$ and DE_N in Fig. 13(l) suggest that the algorithm achieves better enhancement with a bigger local neighbourhood support. However, the plot for CM_N indicates slight performance loss, which is negligible, with high values of w.

3.5. Comparisons with edge-avoiding wavelets based contrast enhancement algorithm

Edge-avoiding wavelet based contrast enhancement algorithm (EAW) [4] achieves global and local contrast enhancement at the same time with a proper parameter selection. Different scale enhancements achieved by modifying the transform domain coefficients reveal details on images. Meanwhile, 2DHE performs a global contrast enhancement. Thus, one expects that EAW outperforms the 2DHE in terms of contrast enhancement. In order to make comparisons, the contrast enhancement results from EAW [4] are utilized in experiments. The *Flower* image [4] shown in Fig. 14(a) is used.

Fig. 14. Contrast enhancement results for image *Flower*. (a, e) Original image. Enhanced images obtained using: (b, f) EAW with medium scale enhancement; (c, g) EAW with fine scale enhancement; and (d, h) 2DHE.

In Fig. 14(b) and (c), the results of EAW are shown for medium and fine scale enhancements. The output of 2DHE is shown in Fig. 14(d). It is clear that EAW produces high contrast output. Meanwhile, 2DHE algorithm also improves the contrast and produces visually pleasing result. The difference in results is caused from the reason that EAW can enhance the details locally, meanwhile 2DHE can only enhance the details globally. However, when the algorithms are applied on a subregion of *Flower* image as shown in Fig. 14(e), it can be observed from Fig. 14(f)–(h) that 2DHE can produce comparable result with respect to EAW at a very low computational requirement.

4. Conclusions

In this paper, we proposed an automatic image enhancement algorithm which employs contextual data modelling using 2D histogram of an input image to perform non-linear data mapping for generating visually pleasing enhancement on different types of images. The proposed algorithm can be applied to both grey-level and colour images with only the size of the spatial neighbour support requiring some tuning. Performance comparisons with state-of-the-art enhancement algorithms show that the proposed algorithm achieves satisfactory image equalization even under diverse illumination conditions. It improves the colour content, brightness and contrast of an image. By achieving high discrete entropy preservation between the input and output images, it preserves the overall content of an input image while providing sufficient contrast enhancement. This is mainly because the proposed algorithm employs contextual information between pixels and their neighbours.

The size of the square local neighbourhood around each pixel determines the performance of the proposed algorithm. The well-known global histogram equalization is a special case of the proposed algorithm when a single pixel with no neighbourhood is used in computing 2D histogram. A metric which combines the discrete entropy with edge based contrast measure is used to automatically estimate the size of the local neighbourhood. It is observed that metric based parameter estimation produces visually pleasing results. However, one can fine tune the local neighbourhood size to achieve different results which brings a flexibility to the proposed algorithm.

The proposed algorithm is simple yet effective for image contrast enhancement. It requires a small number of simple mathematical operations to generate a contrast enhanced image. Thus, it can be applied in real-time applications that require image contrast enhancement while retaining overall image content.

Appendix A. Supplementary data

Supplementary data associated with this article can be found in the online version at doi:http://dx.doi.org.10.1016/j.patcog.2012.03.019.

References

[1] D. Jobson, Z. Rahman, G. Woodell, A multiscale retinex for bridging the gap between color images and the human observation of scenes, IEEE Transactions on Image Processing 6 (7) (1997) 965–976.
[2] S. Agaian, B. Silver, K. Panetta, Transform coefficient histogram-based image enhancement algorithms using contrast entropy, IEEE Transactions on Image Processing 16 (3) (2007) 741–758.
[3] J. Mukherjee, S. Mitra, Enhancement of color images by scaling the DCT coefficients, IEEE Transactions on Image Processing 17 (10) (2008) 1783–1794.
[4] R. Fattal, Edge-avoiding wavelets and their applications, ACM Transactions on Graphics 28 (3) (2009) 1–10.
[5] R.C. Gonzalez, R.E. Woods, Digital Image Processing, 3rd ed., Prentice-Hall, Inc., Upper Saddle River, NJ, USA, 2006.
[6] R. Dale-Jones, T. Tjahjadi, A study and modification of the local histogram equalization algorithm, Pattern Recognition 26 (9) (1993) 1373–1381.
[7] T.K. Kim, J.K. Paik, B.S. Kang, Contrast enhancement system using spatially adaptive histogram equalization with temporal filtering, IEEE Transactions on Consumer Electronics 44 (1) (1998) 82–87.
[8] Y.-T. Kim, Contrast enhancement using brightness preserving bi-histogram equalization, IEEE Transactions on Consumer Electronics 43 (1) (1997) 1–8.
[9] Y. Wang, Q. Chen, B. Zhang, Image enhancement based on equal area dualistic sub-image histogram equalization method, IEEE Transactions on Consumer Electronics 45 (1) (1999) 68–75.
[10] S.-D. Chen, A. Ramli, Minimum mean brightness error bi-histogram equalization in contrast enhancement, IEEE Transactions on Consumer Electronics 49 (4) (2003) 1310–1319.
[11] D. Menotti, L. Najman, J. Facon, A. de Araujo, Multi-histogram equalization methods for contrast enhancement and brightness preserving, IEEE Transactions on Consumer Electronics 53 (3) (2007) 1186–1194.
[12] C.-C. Sun, S.-J. Ruan, M.-C. Shie, T.-W. Pai, Dynamic contrast enhancement based on histogram specification, IEEE Transactions on Consumer Electronics 51 (4) (2005) 1300–1305.
[13] C. Wang, J. Peng, Z. Ye, Flattest histogram specification with accurate brightness preservation, IET Image Processing 2 (5) (2008) 249–262.
[14] T. Arici, S. Dikbas, Y. Altunbasak, A histogram modification framework and its application for image contrast enhancement, IEEE Transactions on Image Processing 18 (9) (2009) 1921–1935.
[15] S. Hashemi, S. Kiani, N. Noroozi, M.E. Moghaddam, An image contrast enhancement method based on genetic algorithm, Pattern Recognition Letters 31 (13) (2010) 1816–1824.
[16] C.E. Shannon, A mathematical theory of communication, Bell System Technical Journal 27 (1948).
[17] A. Beghdadi, A.L. Negrate, Contrast enhancement technique based on local detection of edges, Computer Vision, Graphics, and Image Processing 46 (2) (1989) 162–174.
[18] Retrieved on November 2010 from the World Wide Web 〈http://sipi.usc.edu/database/〉.
[19] Retrieved on November 2010 from the World Wide Web 〈http://r0k.us/graphics/kodak/〉.
[20] D. Martin, C. Fowlkes, D. Tal, J. Malik, A database of human segmented natural images and its application to evaluating segmentation algorithms and measuring ecological statistics, in: Proceedings of 8th International Conference on Computer Vision, vol. 2, 2001, pp. 416–423.

Turgay Celik received the Ph.D. degree in engineering from the University of Warwick, U.K., in 2011. He is currently a research fellow at the Bioinformatics Institute, A*STAR, Singapore. He has produced extensive publications in various international journals and conferences. He has been acting as a reviewer for various international journals and conferences. His research interests are in the areas of biophysics, digital signal, image and video processing, pattern recognition and artificial intelligence, unusual event detection, remote sensing and global optimization techniques.